Flow visualization of Bénard convection using holographic interferometry

Flow visualization of Bénard convection using holographic interferometry

Masahiro Ueda, Kiichiro Kagawa, Koichi Yamada, Chiyozo Yamaguchi, and Yoshifumi Harada

An application of holographic interferometry to Rayleigh-Bénard flow is reported. A fluid seeded with fine alumina particles is illuminated with sheetlike light, and the light scattered from the plane is recorded in a hologram. The reconstructed images give 2-D full-field velocity information within the volume of moving liquid at any instant in time. The convective rolls are regular and oriented perpendicular to the long side of the cell. The vertical velocity distribution closely approximates a sinusoidal function of the horizontal distance and its maximum is nearly proportional to the half-power of the reduced temperature.

I. Introduction

Recently some authors successfully used laser speckle photography to measure the flow velocity of Bénard convection.[1,2] This method, utilizing a thin sheet of laser light, has the feature that it can provide a full-field 2-D velocity distribution in the light sheet at one instant in time.

Another method which can be used to measure the flow velocity is holographic interferometry. This method also uses sheet light and has a full-field nature. An apparent difference between these methods lies in their display, i.e., reconstructed images. The laser speckle method displays images by Young's fringe method from which velocity can be computed or by the spatial filtering method in which an equal velocity component appears.[3] In contrast, holographic interferometry displays images in which each fringe pattern shows an isovelocity region. It is then easy to grasp a general view of flow velocity fields. This feature is favorable especially for observations of the complicated flow field of Bénard convection.

The intent here, however, is not to report a thorough study of the Bénard problem but rather to apply this novel technique known as holographic interferometry to the visualization of Bénard convection flow and illustrate the scope and sensitivity of this method in the course of making a contribution to that problem. A brief comparative study between speckle and holographic methods is also given.

All authors are with Fukui University, Fukui 910, Japan; M. Ueda and K. Kagawa are with the Faculty of Education, the other authors are with the Faculty of Engineering, Department of Applied Physics.

II. Experimental Method

A. Bénard Cell System

A rectangular Bénard cell with interior dimensions of 80 × 40 × 10 mm is constructed for the experiments, a schematic of which is shown in Fig. 1. The cell consists of a 5-mm thick copper plate (a), which is also the top of a lower bath, a 3-mm thick optical glass plate (b), and a 5-mm thick optical glass plate (c). Both upper and lower plates can be maintained at constant temperature by circulating water from the controlled baths above and below the plates, respectively. The cell is filled with glycerol in which fine alumina particles of ~1-μm diam are suspended as light scatterers. Four thermistors T_m attached to the plates near the sidewall are used to determine and control the temperature difference between upper and lower boundaries of the fluid layer through an electric bridge circuit. The potential difference is measured by a digital voltmeter (1 mV = 0.002°C). Plate (b) is an observation window.

In all the experiments the temperature at the lower boundary is maintained constant. The temperature at the upper boundary is maintained at the same value initially, but when it is progressively decreased, the fluid in the cell remains at rest at first until a critical temperature difference ΔT_c is reached where convection takes place. The convection flow just above the critical temperature is anticipated to be a 2-D roll structure

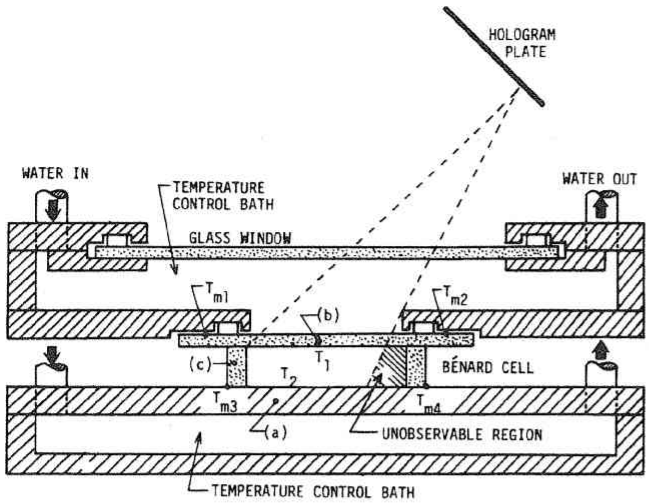

Fig. 1. Schematic section of Bénard cell.

perpendicular to the long side of the cell.[4] If the upper boundary temperature is further reduced, the flow will be more complicated. In this experiment, however, we worked mainly just above the critical temperature ($\Delta T \simeq 1.3\,\Delta T_c$).

B. Holographic Interferometry System

Holographic interferometry has been successfully applied to measurement of flow velocity distributions.[3,5] In this case, a fictitious rough surface is required in the interior of the flowing fluid. For this purpose we seed the fluid with alumina particles and shape the illuminating coherent light into a thin sheet.

Figure 2 is a schematic of the optical system used for this method. In the figure, $\mathbf{s}_i$ is the unit vector in the propagation direction of the sheetlike incident light, and $\mathbf{v}$ is the velocity vector of the particle flow. We make a multiple-exposure hologram with each exposure interval ΔS. The hologram plates H_h and H_v are positioned as shown for horizontal and vertical light sheets, respectively. When a reconstructed image is observed in the direction denoted by a unit vector $\mathbf{s}_o$, interference fringes can be seen in the image of the illuminated plane. The bright interference fringes appear at the position where

$$\mathbf{v} \cdot \Delta S \cdot (\mathbf{s}_o - \mathbf{s}_i) = m\lambda. \tag{1}$$

In the above equation λ is the wavelength, and m is an integer. Equation (1) can be rewritten as

$$V_m = m\lambda/(|\mathbf{s}| \cdot \Delta S), \tag{2}$$

where $\mathbf{s} = \mathbf{s}_o - \mathbf{s}_i$. The symbol V_m denotes the measurable component of the velocity, which is the component along the bisector between $\mathbf{s}_0$ and $\mathbf{s}_i$. The angle θ between $\mathbf{s}_i$ and $\mathbf{b}$, which is the unit vector of the bisector, is $\sim 80°$. Thus, velocity V_m is not an exact vertical velocity component but a close approximation to it (error of $\sim 10°$). This is not very important in a visualization method, but it is more critical in a measurement method of flow velocity distribution. However, if the flow is a simple roll structure as in this experiment, the maximum of V_m will be the maximum velocity of the fluid motion. The maximum of V_m can be obtained in the plane at an appropriate height where the direction of the convective flow velocity coincides with that of V_m.

The optical arrangement used for the experiments is shown in Fig. 3. The light source is an Ar laser, and the wavelength used is 514.5 nm in air. The output power of the laser for the light is ~ 1 W. Multiple pulses with various pulse separations can be obtained by an electromagnetic shutter *EMS*. The sheetlike light is formed through cylindrical lenses CL_1, CL_2, and CL_3. The position of the light sheet is easily changed by shifting lens CL_3 perpendicular to the light in the horizontal plane. A vertical light sheet is formed by the arrangement shown in Fig. 3. A horizontal light sheet can be formed by rotating all the cylindrical lenses 90° in the vertical plane.

III. Results and Discussion

A number of multiple-exposed holograms were recorded for various combinations of light sheet positions and temperature differences. The critical temperature difference ΔT_c was found to be 5.8°C from these experiments. The pulse separations ΔS were 30–130 msec depending on the magnitude of the fluid velocity. The positions of horizontal and vertical light sheets

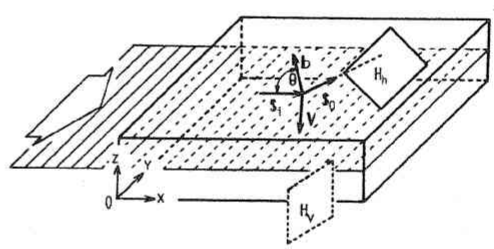

Fig. 2. Optical arrangement for measuring flow velocity distribution by holographic interferometry.

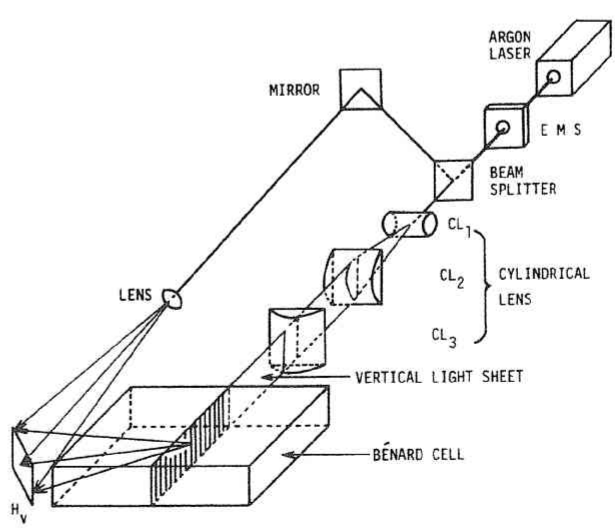

Fig. 3. Optical arrangement used for the experiments.

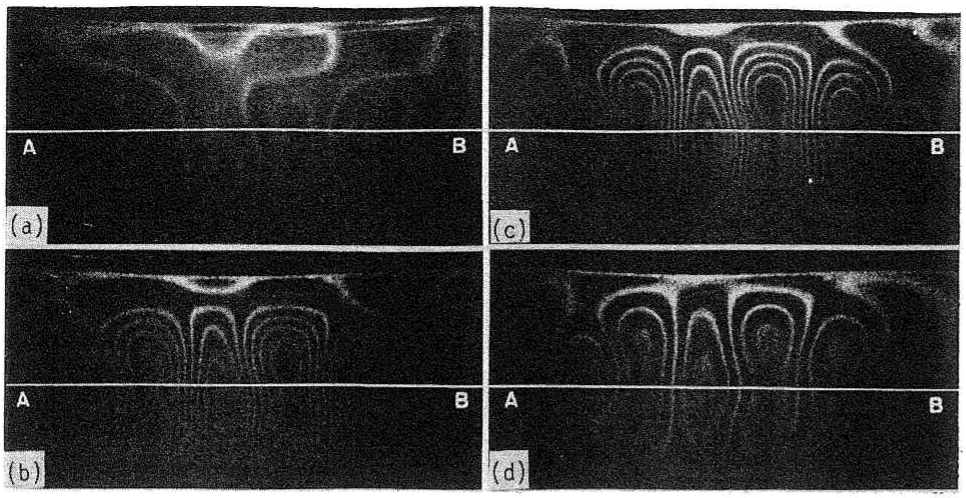

Fig. 4. Reconstructed images for a constant temperature difference $\Delta T/\Delta T_c = 1.204$ in the horizontal section at various heights Z (in millimeters): (a) 2, (b) 4, (c) 6, and (d) 8. In all the figures, one fringe corresponds to a 17.21-μm/sec velocity. A part of the illuminated light sheet cannot be observed because the Bénard system has an unobservable region as shown in Fig. 1.

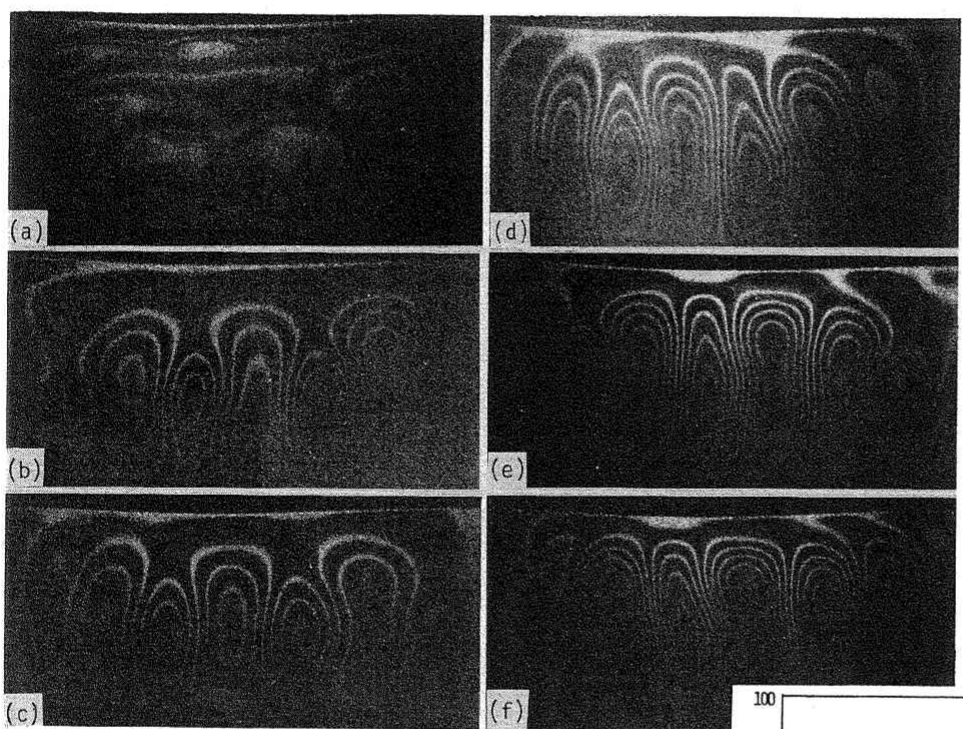

Fig. 5. Reconstructed images for various temperature differences $\Delta T/\Delta T_c$: (a) 0.942, (b) 1.027, (c) 1.089, (d) 1.154, (e) 1.204, and (f) 1.244. All are in the same horizontal section at height Z = 6 mm. One fringe corresponds to velocities of (a) 3.48 μm/sec, (b) 6.77 μm/sec, and (c)–(f) 17.21 μm/sec.

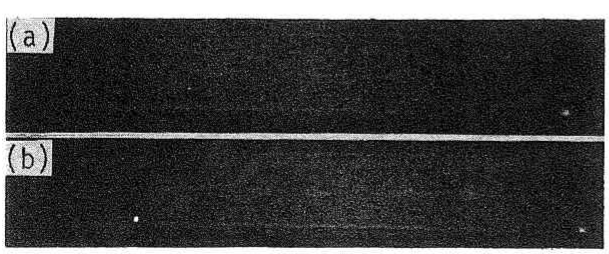

Fig. 6. Reconstructed images in the vertical section at Y = 10 mm for various temperature differences $\Delta T/\Delta T_c$: (a) 1.089 and (b) 1.154. One fringe corresponds to velocities of (a) 6.77 μm/sec and (b) 9.89 μm/sec.

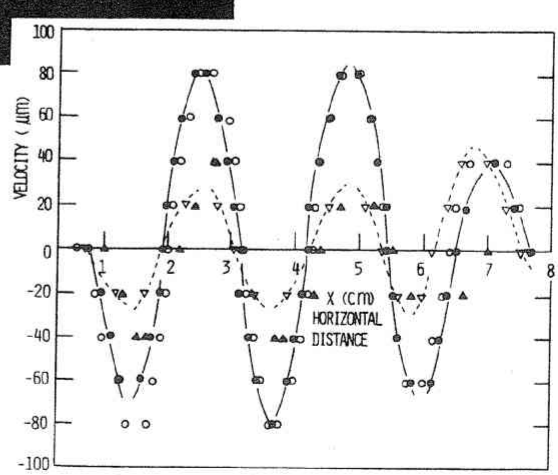

Fig. 7. Flow velocity distribution at various heights Z along line AB in Fig. 4: (a) ▲; (b) ●; (c) ○; (d) ▽.

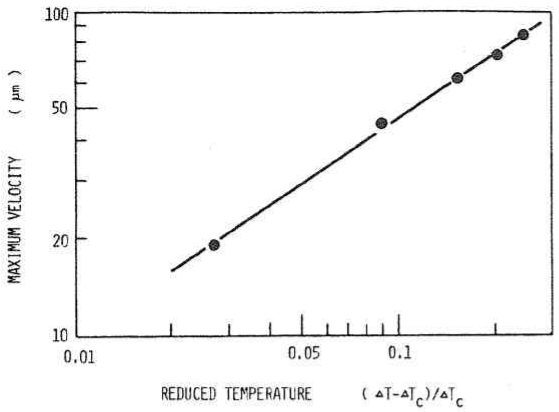

Fig. 8. Maximum vertical velocity vs reduced temperature $\epsilon = \Delta T/\Delta T_c - 1$ in log–log scale.

investigated were $Z = 2, 4, 6$, and 8 mm and $Y = 10$ and 20 mm, respectively (see Fig. 2). The normalized temperature differences were $\Delta T/\Delta T_c = 0.942, 1.027, 1.089, 1.154, 1.204$, and 1.244. The actual temperature at the lower plate was $T_1 = 42.04°C$, and that of the upper plate was decreased very slowly from this value to $T_2 = 34.82°C$.

Examples of the reconstructed images on the horizontal light sheet are shown in Figs. 4 and 5 and those on the vertical light sheet in Fig. 6. The results in Fig. 4 are for a constant temperature difference and the ones in Figs. 5 and 6 for various temperature differences. The pulse separation for Fig. 6 is about twice as long as those for Figs. 4 and 5. It is apparent from these fringe patterns that the 2-D convective rolls are formed with the axis parallel to the short side of the cell. Six distinct rolls are apparent. The fringe pattern in Fig. 6 is attributed to a slight inclination of the bisector **b** to the roll axis. That is, the fringe pattern is not due to the axial velocity component but to the rotating velocity component of the convection roll. Examples of the velocity distribution along line AB in Fig. 4 are shown in Fig. 7. These distributions closely approximate a sinusoidal function of the horizontal distance X. A slight decrease of the velocity near the sidewall is due to a sidewall effect, i.e., a heat transfer through the wall and a frictional force between wall and fluid. Figure 8 shows the relation between a reduced temperature defined by $\epsilon = \Delta T/\Delta T_c - 1$ and the maximum velocity. The results indicate that the maximum velocity is approximately proportional to the half-power of the reduced temperature. This agrees well with the results obtained by Sawada *et al.* for viscous fluid.[6]

In this experiment the maximum velocity was ~100 μm/sec. This is determined by the shortest exposure interval. The interval is restricted by the maximum fringe order m and the exposure time to give sufficient exposure energy required to record a hologram. The energy scattered by the suspended particles onto the hologram strongly depends on the particle size, particle concentration, and distance from the scatterer to the hologram. In the optical arrangement shown in Fig. 3 the laser of 1-W output power makes the interval as short as 20 msec. If we assume an optical system of $|\mathbf{s}| = 1$ and a fifth-order fringe, the pulse separation of this laser allows us to measure velocity up to ~0.13 mm/sec, as seen from Eq. (2). We can measure faster velocity than this value if the multiple-exposure method is used as in this experiment. If the flow is unsteady, the number of exposures, however, must be chosen in such a way that the temporal velocity variations are low within the total duration of the exposure.

In the measurement by speckle photography the observation direction must be perpendicular to the light sheet to prevent the movement of the speckle by a spatial gradient.[7] The intensity of light scattered in this direction is very weak. By contrast, we can use a strong forward scattering light in the holographic interferometry as shown in Figs. 2 and 3. The pulse duration can then be extremely shortened.

IV. Conclusions

Holographic interferometry has been demonstrated to be capable of full-field velocity measurements of Rayleigh-Bénard flow. The measurements show that (1) a 2-D roll pattern is established with the roll axis perpendicular to the long side of the cell in the range just above the critical temperature, (2) the vertical velocity distribution is of sinusoidal form with respect to the horizontal distance, and (3) the maximum vertical velocity is nearly proportional to the half-power of the reduced temperature.

Our initial works have shown that holographic interferometry has some advantages over speckle photography in the study of fluid dynamic problems. When comparing these methods, it is possible that whole flow velocity fields may be easier to see by the holographic method than by speckle photography. Further, holographic interferometry enables us to measure faster velocity, provided that the laser power and the variables of the other optical system are roughly the same in both methods. The speckle photography, however, has the advantage that it can give more information: it can give two velocity components simultaneously.

One of the authors (M.U.) would like to thank K. Iwata of Osaka Prefecture University for his helpful discussions during the performance of the experiments.

References

1. P. G. Simpkins and T. D. Dudderar, J. Fluid Mech. **89**, Part 4, 665 (1978).
2. R. Meynart, Proc. Soc. Photo-Opt. Instrum. Eng. **210**, 25 (1979).
3. K. Iwata, "Fundamental Studies of Optical Methods for Measuring Three-Dimensional Distribution of Flow Velocity," Thesis, Osaka U., Japan (1980).
4. E. L. Koschmieder, Adv. Chem. Phys. **26**, 177 (1974).
5. K. Iwata, T. Hakoshima, and R. Nagata, J. Opt. Soc. Am. **67**, 117 (1977).
6. Sawada *et al.* private communication (1981).
7. F. P. Chiang and R. M. Juang, Appl. Opt. **15**, 2199 (1976).